

Supplementary data for

Effect of incubation conditions on hemolytic properties of the unmodified graphene oxide with various concentrations

Yang Wang¹, Baomei Zhang¹, Guangxi Zhai^{1*}

¹ Department of Pharmaceutics, College of Pharmaceutical Sciences, Shandong University, Jinan 250012, China

* Author to whom correspondence should be addressed.

Guangxi Zhai, Ph D, Professor

Tel.: (86) 531-88382015

E-mail: professorgxzhai @126.com

Supporting Contents

Information S1 The fitting of three sets of binary linear equations	S2
Information S2 Comparison of calculation methods of hemolysis percentage	S5
Information S3 Surface area calculation of RBCs and GO	S7
Information S4 The shear stress exerted on RBCs membrane	S9
Information S5 The number calculation of GO nanosheets	S12
Figure S1 The color of GO colloidal solutions	S13
Figure S2 The physicochemical characterizations of GO	S13
Figure S3 Typical photos of rabbit RBCs after incubation	S14
Figure S4 The heme concentration curves in two incubation medium	S15
Figure S5 The effect of RBCs species on hemolysis properties of GO	S15
Figure S6 The effect of RBCs concentration on hemolysis assays of GO	S16
Figure S7 The storage effect of RBCs on hemolysis assays of GO	S16
Figure S8 The health status effect of RBCs on hemolysis properties of GO	S17
Figure S9 The centrifugal effect on hemolysis of GO	S17
Figure S10 The heme concentration curves for the time from 0 h to 24h	S18
Figure S11 The incubation temperature effect on hemolysis of GO	S18
Figure S12 The incubation temperature effect on hemolysis of GO	S19
References	S19

Information S1 The fitting of three sets of binary linear equations

The three sets of binary linear algebraic equations for rabbits, guinea pigs and rats were fitted by Matlab software, respectively.

(1) For rabbits:

The actual concentration of heme and GO and actual absorption differences were as below.

Actual concentration		Actual absorption differences*		Fitted heme concentration	Deviation
Heme ($\mu\text{mol L}^{-1}$)	GO ($\mu\text{g mL}^{-1}$)	$A_{540}-A_{600}$	$A_{576}-A_{600}$	($\mu\text{mol L}^{-1}$)	(%)
2.83	0	0.034	0.037	2.6136	-7.52
5.14	0	0.064	0.069	4.9069	-4.63
9.78	0	0.125	0.135	9.6419	-1.44
19.64	0	0.252	0.273	19.545	-0.47
28.41	0	0.366	0.395	28.291	-0.40
37.10	0	0.478	0.517	37.048	-0.14
45.58	0	0.588	0.636	45.585	0.01
5	10	0.081	0.072	5.0413	0.83
10	10	0.140	0.135	9.5567	-4.43
20	10	0.275	0.279	19.877	-0.62
30	10	0.406	0.421	30.065	0.22
40	10	0.536	0.561	40.106	0.27
50	10	0.659	0.694	49.647	-0.71
60	10	0.787	0.836	59.853	-0.24
5	50	0.130	0.079	5.3019	6.04
10	50	0.206	0.145	9.9516	-0.48
20	50	0.343	0.288	20.183	0.91
30	50	0.476	0.431	30.438	1.46
40	50	0.609	0.575	40.769	1.92
50	50	0.736	0.713	50.673	1.35
60	50	0.864	0.853	60.724	1.21
5	100	0.190	0.096	6.2698	25.40
10	100	0.245	0.143	9.576	-4.24
20	100	0.397	0.277	19.03	-4.85
30	100	0.544	0.430	29.974	-0.09
40	100	0.673	0.569	39.943	-0.14
50	100	0.797	0.705	49.71	-0.58
60	100	0.912	0.834	58.989	-1.69

*: the differences were the means of three repeated samples.

For rabbits:

The set of binary linear algebraic equations fitted by Matlab software was as

below.

$$A_{540}-A_{600}=0.01317*C_{\text{heme}} + 0.001412*C_{\text{GO}} - 0.004156$$

$$A_{576}-A_{600}=0.01396*C_{\text{heme}} + 0.0001042*C_{\text{GO}} + 0.0002387$$

Deviation was calculated as follows:

$$\text{deviation (\%)} = \frac{C_{\text{heme}}^{\text{fitted}} - C_{\text{heme}}^{\text{actual}}}{C_{\text{heme}}^{\text{actual}}} \times 100$$

The mean deviation of fitted and actual heme concentrations was calculated as follows:

$$\text{mean deviation (\%)} = \frac{|\text{Deviation}_1| + |\text{Deviation}_2| + \dots + |\text{Deviation}_n|}{n} \times 100$$

The mean deviation for rabbit RBCs was 2.58%.

(2) For guinea pigs:

The actual concentration of heme and GO and actual absorption differences were as below.

Actual concentration		Actual absorption differences*		Fitted heme concentration ($\mu\text{mol L}^{-1}$)	Deviation (%)
Heme ($\mu\text{mol L}^{-1}$)	GO ($\mu\text{g mL}^{-1}$)	$A_{540}-A_{600}$	$A_{576}-A_{600}$		
2.44	0.00	0.023	0.018	2.5401	4.12
4.88	0.00	0.050	0.041	5.405	10.78
9.76	0.00	0.096	0.079	10.031	2.79
19.52	0.00	0.189	0.155	19.207	-1.59
29.28	0.00	0.284	0.233	28.658	-2.11
39.03	0.00	0.379	0.312	38.324	-1.82
48.79	0.00	0.412	0.308	34.923	-28.43
2.44	10.00	0.060	0.032	2.7002	10.68
4.88	10.00	0.090	0.056	5.549	13.73
9.76	10.00	0.137	0.098	10.958	12.29
19.52	10.00	0.234	0.181	21.33	9.29
29.28	10.00	0.333	0.267	32.193	9.97
39.03	10.00	0.432	0.352	42.841	9.75
48.79	10.00	0.530	0.436	53.351	9.34
2.44	50.00	0.169	0.071	2.6896	10.25
4.88	50.00	0.194	0.087	4.2038	-13.84
9.76	50.00	0.249	0.127	8.5668	-12.21
19.52	50.00	0.381	0.224	19.253	-1.35
29.28	50.00	0.478	0.309	30.055	2.66

39.03	50.00	0.573	0.393	40.796	4.51
48.79	50.00	0.664	0.474	51.201	4.94
2.44	80.00	0.239	0.092	1.813	-25.68
4.88	80.00	0.269	0.113	4.017	-17.67
9.76	80.00	0.315	0.147	7.7833	-20.24
19.52	80.00	0.448	0.240	17.533	-10.17
29.28	80.00	0.574	0.336	28.466	-2.76
39.03	80.00	0.673	0.424	39.759	1.86
48.79	80.00	0.759	0.504	50.333	3.16

*: the differences were the means of three repeated samples

For guinea pigs:

The set of binary linear algebraic equations fitted by Matlab software was as below.

$$A_{540}-A_{600}=0.01032*C_{\text{heme}}+0.003224*C_{\text{GO}}-0.009742$$

$$A_{576}-A_{600}=0.008349*C_{\text{heme}}+0.001155*C_{\text{GO}}-0.005546$$

The mean deviation for guinea pig RBCs was 9.21%.

(3) For rats:

The actual concentration of heme and GO and actual absorption differences were as below.

Actual concentration		Actual absorption differences*		Fitted heme concentration ($\mu\text{mol L}^{-1}$)	Deviation (%)
Heme ($\mu\text{mol L}^{-1}$)	GO ($\mu\text{g mL}^{-1}$)	$A_{540}-A_{600}$	$A_{576}-A_{600}$		
10.70	0.00	0.126	0.133	10.583	-1.10
21.40	0.00	0.266	0.282	23.761	11.03
42.80	0.00	0.511	0.541	46.654	9.00
85.60	0.00	0.996	1.056	92.191	7.69
2.68	10.00	0.053	0.033	1.59	-40.56
5.35	10.00	0.088	0.063	4.1944	-21.60
10.70	10.00	0.144	0.122	9.4082	-12.08
21.40	10.00	0.251	0.235	19.396	-9.37
32.10	10.00	0.362	0.353	29.83	-7.08
42.80	10.00	0.472	0.470	40.177	-6.13
53.50	10.00	0.581	0.585	50.34	-5.91
2.68	50.00	0.165	0.072	4.5005	68.24
5.35	50.00	0.190	0.095	6.5103	21.68
10.70	50.00	0.237	0.139	10.361	-3.17
21.40	50.00	0.365	0.252	20.198	-5.62
32.10	50.00	0.502	0.378	31.208	-2.78

42.80	50.00	0.612	0.494	41.46	-3.14
53.50	50.00	0.720	0.611	51.821	-3.14
2.68	80.00	0.242	0.099	6.5193	143.70
5.35	80.00	0.267	0.121	8.4339	57.64
10.70	80.00	0.319	0.166	12.344	15.36
21.40	80.00	0.427	0.263	20.802	-2.80
32.10	80.00	0.545	0.373	30.425	-5.22
42.80	80.00	0.678	0.497	41.274	-3.57
53.50	80.00	0.793	0.617	51.87	-3.05

*: the differences were the means of three repeated samples

For rats:

$$A_{540}-A_{600}=0.01119*C_{\text{heme}}+0.002455*C_{\text{GO}}+0.002146$$

$$A_{576}-A_{600}=0.01135*C_{\text{heme}}+0.0001844*C_{\text{GO}}+0.01247$$

The mean deviation for guinea pig RBCs was 19.83%.

Information S2 Comparison of calculation methods of hemolysis percentage

The hemolytic activity of GO was investigated at two-point absorbance at 540 nm and 655 nm by Singh *et al*¹ and Liao *et al*.² The method called the 540-655 method hereafter. Moreover, the hemolytic activity was also compared the calculation results of absorbance at 540 nm³⁻⁹. This method was called 540 method. Certainly, there were other methods reported by measurement of absorption at 541 nm^{10, 11}, 542 nm¹², 545 nm¹³⁻¹⁸ or 570 nm¹⁹ in the previous studies. The novel 540-576-600 method was only compared with the two typical 540-655 method and 540 method here because the two methods were frequently employed by the previous documents.

(1) For 540-655 method:

The hemolysis percentage equation was as below.

$$\text{hemolysis}(\%) = \frac{(A_{540}^{\text{sample}} - A_{655}^{\text{sample}}) - (A_{540}^{\text{neg}} - A_{655}^{\text{neg}})}{(A_{540}^{\text{pos}} - A_{655}^{\text{pos}}) - (A_{540}^{\text{neg}} - A_{655}^{\text{neg}})} \times 100$$

(2) For 540 method:

The hemolysis percentage equation was as below.

$$\text{hemolysis}(\%) = \frac{A_{540}^{\text{sample}} - A_{540}^{\text{neg}}}{A_{540}^{\text{pos}} - A_{540}^{\text{neg}}} \times 100$$

In order to show the superiority of our 540-576-600 method to the other two methods, rats RBCs (in the section of 2.4 RBCs species) was as a typical example (the hemolysis photo in Figure 2a) and three methods were compared together as below.

Table The results of hemolysis from rat RBCs

	540 method		540-655 method		540-576-600 method	
	Mean(%)	SD(%)	Mean(%)	SD(%)	Mean(%)	SD(%)
neg	0.00	1.91	0.00	1.17	0.00	0.21
5 $\mu\text{g mL}^{-1}$	8.04	1.82	0.67	1.97	-0.55	0.34
10 $\mu\text{g mL}^{-1}$	21.29	2.69	3.20	2.23	-0.86	0.36
15 $\mu\text{g mL}^{-1}$	30.34	3.92	5.27	3.56	-1.04	0.55
20 $\mu\text{g mL}^{-1}$	38.76	2.61	6.80	2.02	-1.24	0.32
25 $\mu\text{g mL}^{-1}$	50.94	1.86	11.93	1.56	-0.88	0.26
30 $\mu\text{g mL}^{-1}$	60.93	4.13	15.87	2.39	-0.66	0.33
40 $\mu\text{g mL}^{-1}$	80.34	6.12	22.87	3.25	-0.35	0.41
50 $\mu\text{g mL}^{-1}$	99.37	3.06	30.40	2.21	0.03	0.30
75 $\mu\text{g mL}^{-1}$	159.99	9.11	54.07	4.92	1.52	0.54
100 $\mu\text{g mL}^{-1}$	222.49	11.29	78.67	5.44	3.08	0.59
pos	100.00	9.47	100.00	9.24	17.34	1.59

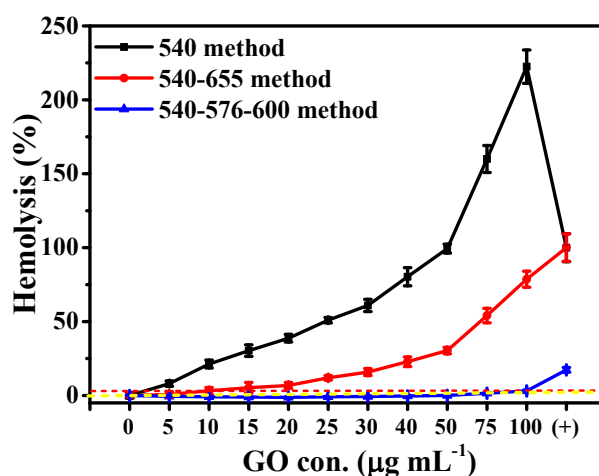


Figure the comparison of hemolytic percentages from rat RBCs

In 540 method, the hemolysis percentages was continuously and drastically increased from 0 to 222 % with change of GO concentration. The hemolysis modestly boost to 78% in 540-655 method, while there was little increase in 540-576-600 method (from $-0.55 \pm 0.34\%$ to $3.08 \pm 0.59\%$ for GO from 5 to 100 $\mu\text{g mL}^{-1}$).

Another example was rabbit RBCs in isotonic glucose solution (in the section of

2.3 Medium type). Three methods were compared together in the below figure.

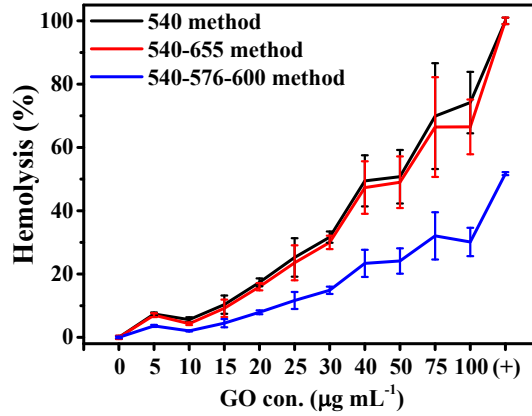


Figure The comparison of hemolysis from rabbit RBCs.

From the two examples, the 540-576-600 method was superior to the other methods because of avoidance of false-positive errors.

Information S3 Surface area calculation of RBCs and GO

(1) Surface area calculation of RBCs

The surface area and volume of one rabbit RBCs were $96.7 \pm 10.2 \mu\text{m}^2$ and $60.9 \pm 12 \mu\text{m}^3$, respectively,²⁰ so 1% RBCs was about $1.64 \times 10^8 \text{ cells mL}^{-1}$, and the total calculated surface area of 1% RBCs was $15.9 \times 10^{-3} \text{ m}^2 \text{ mL}^{-1}$. Similarly, the surface area of 0.5%, 0.75% 1.5% and 2% RBCs were 7.95, 11.925, 23.85 and $31.8 \times 10^{-3} \text{ m}^2 \text{ mL}^{-1}$, respectively. The calculation procedure was as below.

(i) For 1% rabbit RBCs suspensions,

$$\text{the total cell count} = \frac{1\text{mL} \times 1\%}{60.9 \mu\text{m}^3 / \text{cell}} = \frac{1 \times 10^{-6} \text{m}^3 \times 1\%}{60.9 \times 10^{-18} \text{m}^3 / \text{cell}} = 1.64 \times 10^8 \text{ cells}$$

$$\text{surface area} = 1.64 \times 10^8 \text{ cells} \times 96.7 \mu\text{m}^2 \text{ cells}^{-1} = 15.9 \times 10^{-3} \text{ m}^2 \text{ mL}^{-1}$$

(ii) For 0.5% rabbit RBCs suspensions,

$$\text{surface area} = 1.64 \times 10^8 \text{ cells} \times \frac{1}{2} \times 96.7 \mu\text{m}^2 \text{ cells}^{-1} = 7.95 \times 10^{-3} \text{ m}^2 \text{ mL}^{-1}$$

(iii) For 0.75% rabbit RBCs suspensions,

$$\text{surface area} = 1.64 \times 10^8 \text{ cells} \times \frac{3}{4} \times 96.7 \mu\text{m}^2 \text{ cells}^{-1} = 11.925 \times 10^{-3} \text{ m}^2 \text{ mL}^{-1}$$

(iv) For 1.5% rabbit RBCs suspensions,

$$\text{surface area} = 1.64 \times 10^8 \text{ cells} \times \frac{3}{2} \times 96.7 \mu\text{m}^2 \text{ cells}^{-1} = 23.85 \times 10^{-3} \text{ m}^2 \text{ mL}^{-1}$$

(v) For 2% rabbit RBCs suspensions,

$$\text{surface area} = 1.64 \times 10^8 \text{ cells} \times 2 \times 96.7 \mu\text{m}^2 \text{ cells}^{-1} = 31.8 \times 10^{-3} \text{ m}^2 \text{ mL}^{-1}$$

(2) Surface area calculation of GO

The specific surface area of GO nanosheets experimentally measured by diluted GO solutions was $736.6 \text{ m}^2 \text{ g}^{-1}$, and for GO concentration of $50 \mu\text{g mL}^{-1}$, the estimated aggregation levels were 15%²¹. The calculated surface area of GO at 10, 20, 30, 40 and $50 \mu\text{g mL}^{-1}$ were about 7.37, 14.73, 22.10, 29.46 and $31.31 \times 10^{-3} \text{ m}^2 \text{ mL}^{-1}$, respectively.

(i) For $10 \mu\text{g mL}^{-1}$ GO,

$$\text{surface area} = 736.6 \text{ m}^2 \text{ g}^{-1} \times 10 \mu\text{g mL}^{-1} = 7.366 \times 10^{-3} \text{ m}^2 \text{ mL}^{-1} \approx 7.37 \times 10^{-3} \text{ m}^2 \text{ mL}^{-1}$$

(ii) For $20 \mu\text{g mL}^{-1}$ GO,

$$\text{surface area} = 736.6 \text{ m}^2 \cdot \text{g}^{-1} \times 20 \mu\text{g mL}^{-1} \approx 14.73 \times 10^{-3} \text{ m}^2 \text{ mL}^{-1}$$

(iii) For $30 \mu\text{g mL}^{-1}$ GO,

$$\text{surface area} = 736.6 \text{ m}^2 \text{ g}^{-1} \times 30 \mu\text{g mL}^{-1} \approx 22.10 \times 10^{-3} \text{ m}^2 \text{ mL}^{-1}$$

(iv) For $40 \mu\text{g mL}^{-1}$ GO,

$$\text{surface area} = 736.6 \text{ m}^2 \text{ g}^{-1} \times 40 \mu\text{g mL}^{-1} \approx 29.46 \times 10^{-3} \text{ m}^2 \text{ mL}^{-1}$$

(v) For $50 \mu\text{g mL}^{-1}$ GO,

$$\text{surface area} = 736.6 \text{ m}^2 \text{ g}^{-1} \times 50 \mu\text{g mL}^{-1} \times (1 - 15\%) \approx 31.31 \times 10^{-3} \text{ m}^2 \text{ mL}^{-1}$$

(3) the needed GO and the used Hb concentration

According to the guideline of ASTM F-756-00, the needed GO and the used Hb concentration in the assay was calculated as below.

$$\text{needed GO concentration} = \frac{21 \times 10^{-4} \text{ m}^2 / 8 \text{ mL}}{736.6 \text{ m}^2 / \text{g}} = 3.56 \times 10^{-7} \text{ g mL}^{-1} = 0.356 \mu\text{g mL}^{-1}$$

$$\text{used Hb concentration} = \frac{(185.84 \pm 6.31 \mu\text{mol L}^{-1}) \times 69737 \text{ g mol}^{-1}}{4} = 3.24 \pm 0.11 \text{ mg mL}^{-1}$$

In which 21 cm^2 (equal to $21 \times 10^{-4} \text{ m}^2$) was the needed surface area of materials;

8 mL was the total suspensions volume containing materials and RBCs;

$736.6 \text{ m}^2 \text{ g}^{-1}$ was the measured value of GO specific surface area.

$185.84 \pm 6.31 \mu\text{mol L}^{-1}$ was the $C_{\text{total Heme}}$ for 1% of hematocrit in rabbit

RBCs suspension;

69737 g mol⁻¹ was molecular weight of Hb from rabbits (PDB ID: 2RAO, seen the website: <http://www.rcsb.org/pdb/home/home.do>);

4 was the molar ratio between heme and Hb.

(4) The used rabbit RBCs hematocrit recommended by ASTM

In 7 mL of PBS solution with samples, the added volume was 1 mL blood with containing the total hemoglobin content of 10 ± 1 mg mL⁻¹. So the total volume of RBCs suspension was 8 mL. Additionally, the hematocrit of healthy rabbit blood was 37.41%²².

The final adding volume of whole blood was as below:

$$\text{final adding volume of whole blood} = \frac{1\% \times (10 \pm 1) \text{ mg mL}^{-1}}{\frac{37.81\%}{8\text{mL}} \times 3.24 \pm 0.1 \text{ mg mL}^{-1}} \approx 0.66\text{mL}$$

The final RBCs hematocrit recommended by ASTM was as below:

$$\text{final hematocrit} = \frac{1\% \times (10 \pm 1) \text{ mg mL}^{-1}}{3.24 \pm 0.1 \text{ mg mL}^{-1}} \approx 3.1\%$$

(5) The GO concentration recommended by ASTM

The final RBCs hematocrit recommended by ASTM was 3.1 %

the GO surface area needed in the assay was 0.356 μg mL⁻¹

When the hematocrit of RBCs was set 1%, the recommended GO concentration was proportionally as below:

$$\text{recommended GO concentration} = \frac{1\%}{3.1\%} \times 0.356 \mu\text{g mL}^{-1} \approx 0.115 \mu\text{g mL}^{-1}$$

Information S4 The shear stress exerted on RBCs membrane

The calculation procedure was seen as below.

(1) The relationship of rotational speed (N) and relative centrifugal force (RCF) was as below.

$$RCF = r \times \omega^2 / g$$

Where g is earth's gravitational acceleration,

r is the rotational radius,

ω is the angular velocity in radians per unit time.

This relationship may be written as

$$RCF = 1.11824396 \times 10^{-6} N^2 r_{\text{mm}}$$

Where r_{mm} is the rotational radius measured in millimeters (mm),

N is rotational speed measured in revolutions per minute (rpm).

The different rotational speed (N) was corresponded to the following relative centrifugal force (RCF) for high speed centrifuge (HC-2062, Anhui HSTC Zonkia Scientific Instruments Co. Ltd., Anhui, China).

N (rpm)	1000	2000	3000	4000	6000	8000
RCF (g)	67	268	603	1072	2412	4288

Note: the unit of RCF was N/kg.

(2) The mass of GO nanosheets was calculated as below.

For mean mass:

$$\text{mean mass of GO} = \frac{\text{surface area}}{\text{specific surface area}} = \frac{54991 \text{ nm}^2}{736.6 \text{ m}^2 \text{ g}^{-1}} \approx 74.66 \times 10^{-21} \text{ kg sheet}^{-1}$$

Where 54991 nm^2 was the mean area of GO nanosheets

For minimal mass:

$$\text{minimal mass of GO} = \frac{977 \text{ nm}^2}{736.6 \text{ m}^2 \text{ g}^{-1}} \approx 1.33 \times 10^{-21} \text{ kg sheet}^{-1}$$

Where 977 nm^2 was the minimal area of GO nanosheets

For maximal mass:

$$\text{maximal mass of GO} = \frac{793945 \text{ nm}^2}{736.6 \text{ m}^2 \text{ g}^{-1}} \approx 1077.85 \times 10^{-21} \text{ kg sheet}^{-1}$$

Where 793945 nm^2 was the maximal area of GO nanosheets

(3) The centrifugal force of GO exerted on RBCs membrane

For mean centrifugal force at rotational speed of 1000 rpm:

$$\text{mean force} = RCF \cdot m = 67 \times 74.66 \times 10^{-21} \text{ kg sheet}^{-1} \approx 5.00 \times 10^{-18} \text{ N sheet}^{-1}$$

For minimal centrifugal force at rotational speed of 1000 rpm:

minimal centrifugal force of GO = $67 \times 1.33 \times 10^{-21} \text{ kg sheet}^{-1} \approx 0.09 \times 10^{-18} \text{ N sheet}^{-1}$

For maximal centrifugal force at rotational speed of 1000 rpm:

maximal centrifugal force of GO = $67 \times 1077.85 \times 10^{-21} \text{ kg sheet}^{-1} \approx 72.22 \times 10^{-18} \text{ N sheet}^{-1}$

The different centrifugal forces corresponded to rotational speeds were listed as below.

<i>N</i> (rpm)	Minimum ($\times 10^{-18} \text{ N sheet}^{-1}$)	Mean ($\times 10^{-18} \text{ N sheet}^{-1}$)	Maximum ($\times 10^{-18} \text{ N sheet}^{-1}$)
1000	0.09	5.00	72.22
2000	0.36	20.01	288.86
3000	0.80	45.02	649.94
4000	1.43	80.04	1155.46
6000	3.21	180.08	2599.77
8000	5.70	320.14	4621.82

Note: the data was theoretically the centrifugal force produced by single GO sheet

(4) Shear stress of GO nanosheets on RBCs membrane

For GO nanosheets, the thickness was about 1 nm, but the contact length was unknown, so the contact area was unknown. Supposing the contact length was 10 nm, contact area was approximately 10 nm^2 . Then the shear stress was calculated as below.

For mean shear stress at rotational speed of 1000 rpm:

$$\text{mean shear stress of GO} = \frac{F}{A} = \frac{5.00 \times 10^{-18} \text{ N sheet}^{-1}}{10 \text{ nm}^2} = 0.5 \text{ Pa sheet}^{-1}$$

For minimal shear stress at rotational speed of 1000 rpm:

$$\text{minimal shear stress of GO} = \frac{0.09 \times 10^{-18} \text{ N sheet}^{-1}}{10 \text{ nm}^2} = 0.009 \text{ Pa sheet}^{-1}$$

For maximal shear stress at rotational speed of 1000 rpm:

$$\text{maximal shear stress of GO} = \frac{72.22 \times 10^{-18} \text{ N sheet}^{-1}}{10 \text{ nm}^2} = 7.22 \text{ Pa sheet}^{-1}$$

The shear stress corresponded to rotational speeds were listed as below.

<i>N</i> (rpm)	Minimum (Pa sheet^{-1})	Mean (Pa sheet^{-1})	Maximum (Pa sheet^{-1})
1000	0.009	0.5	7.222
2000	0.036	2.001	28.886
3000	0.08	4.502	64.994
4000	0.143	8.004	115.546
6000	0.321	18.008	259.977

8000

0.57

32.014

462.182

Note: the data was theoretically the shear force produced by single GO sheet

(5) The comparison of shear stress

According to the previous report,²³ the measured threshold of RBCs was 1500 dynes cm⁻², namely, 150 Pa. While the shear stress produced by a single GO sheet via centrifugation was various owing to the difference of GO size. Compared these data, the shear stress was above the threshold if the size of GO nanosheets was large and centrifugation speed was high. For example, the shear stress of GO nanosheets with the maximal surface area at 6000 rpm was about 260 Pa, which far exceeded the threshold of 150 Pa.

Information S5 The number calculation of GO nanosheets

The mean surface area of GO nanosheets was 54991 nm², which was obtained by AFM NanoScope analysis software. So the number of GO nanosheets was theoretically calculated followed. Due to massive aggregation of GO when GO concentration was more than 35 µg·mL⁻¹, the actual number of GO nanosheets with mid and high concentration was less than the theoretical values calculated above.

(i) For low GO concentration (10 µg mL⁻¹),

$$\text{number of GO} = \frac{736.6 \text{ m}^2 \text{ g}^{-1} \times 10 \mu\text{g mL}^{-1}}{54991 \text{ nm}^2} \approx 1.339 \times 10^{11} \text{ sheets mL}^{-1}$$

(ii) For mid GO concentration (40 µg mL⁻¹),

$$\text{number of GO} = \frac{736.6 \text{ m}^2 \text{ g}^{-1} \times 40 \mu\text{g mL}^{-1}}{54991 \text{ nm}^2} \approx 5.356 \times 10^{11} \text{ sheets mL}^{-1}$$

(iii) For high GO concentration (80 µg mL⁻¹),

$$\text{number of GO} = \frac{736.6 \text{ m}^2 \text{ g}^{-1} \times 80 \mu\text{g mL}^{-1}}{54991 \text{ nm}^2} \approx 10.712 \times 10^{11} \text{ sheets mL}^{-1}$$

Supporting Figure

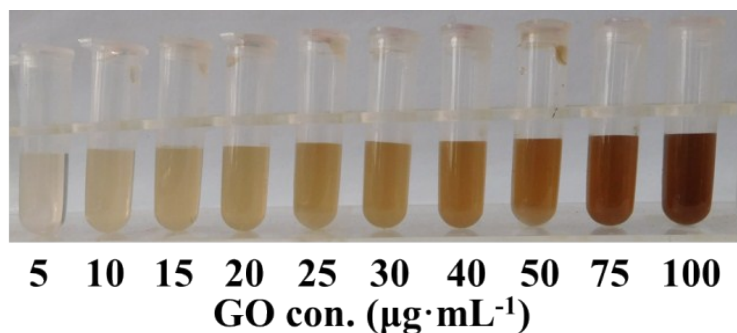


Figure S1. The brown color of GO colloidal solutions was became more brown with increasing concentration from 5 to 100 $\mu\text{g mL}^{-1}$.

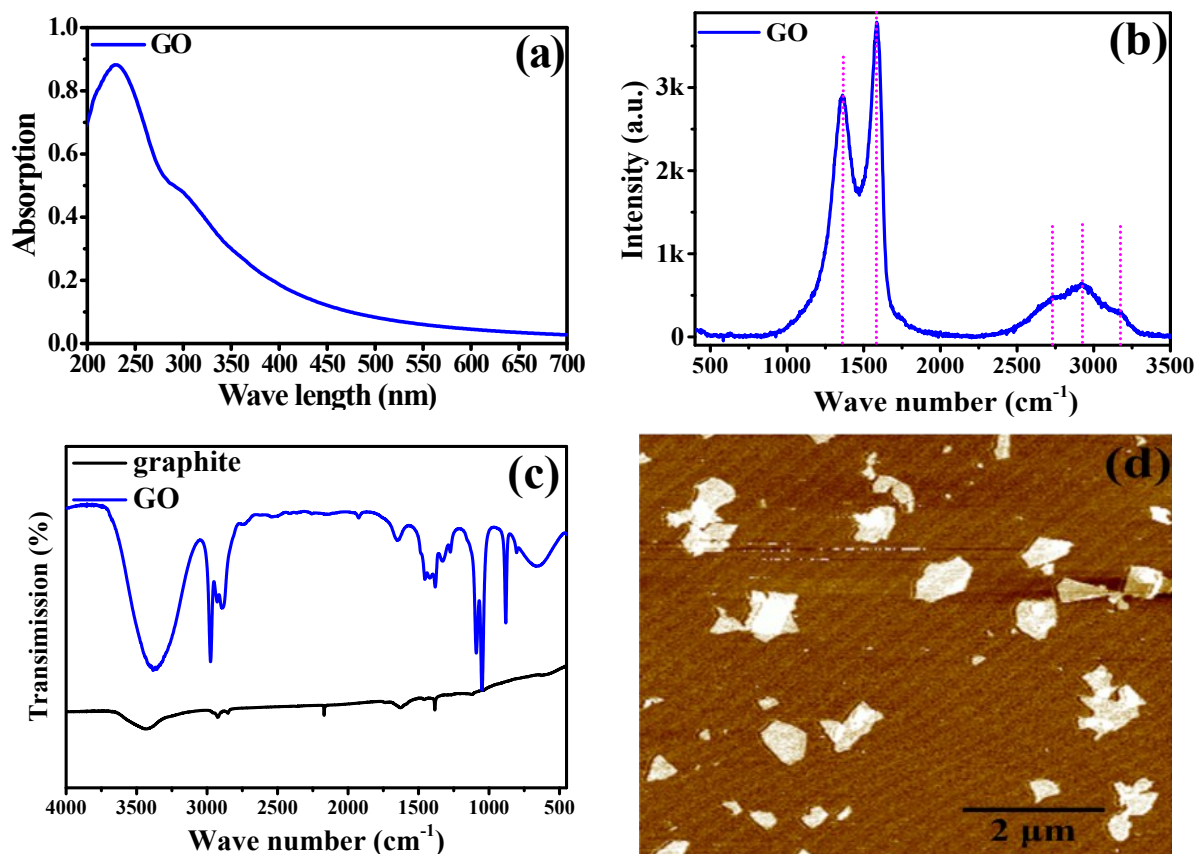


Figure S2. The physicochemical characterizations of as-prepared GO nanosheets. (a) UV spectrum of GO nanosheets, (b) Raman spectrum of GO nanosheets, (c) FTIR spectrum of GO nanosheets, (d) AFM of GO nanosheets (scale bar represented 2 μm). In the 2D images of GO, brown color represented mica substrate and white region represented GO.

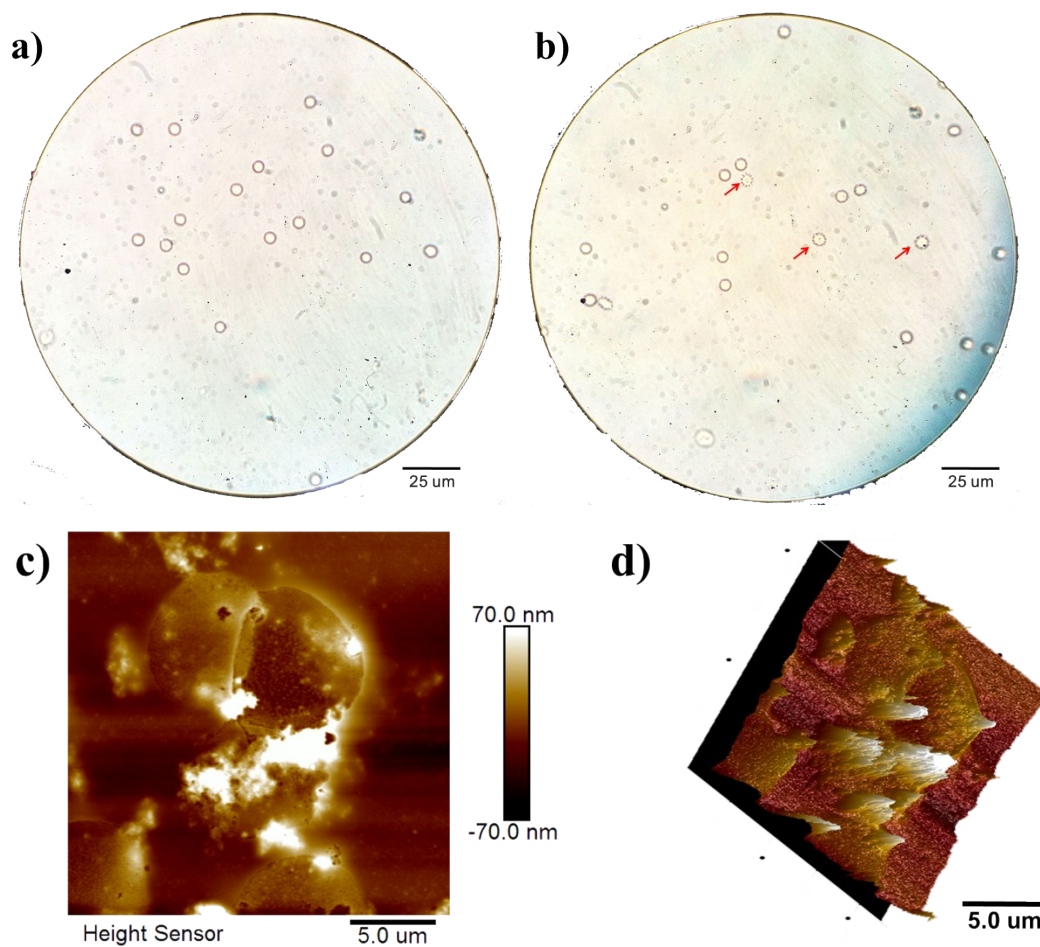


Figure S3. Typical photos of rabbit RBCs after incubation of 1% RBCs with $40\mu\text{g mL}^{-1}$ GO at $37\text{ }^{\circ}\text{C}$ for 3h. (a) rabbit RBCs in PBS by Alphaphot-2 YS2-H light microscope (Nikon, Japan), (b) rabbit RBCs in 5% glucose solution by ordinary microscopes (the red lines showed the rupturing RBCs); (c) 2D graph of rabbit RBCs in 5% glucose solution by AFM; (d) 3D graph of rabbit RBCs in 5% glucose solution by AFM.

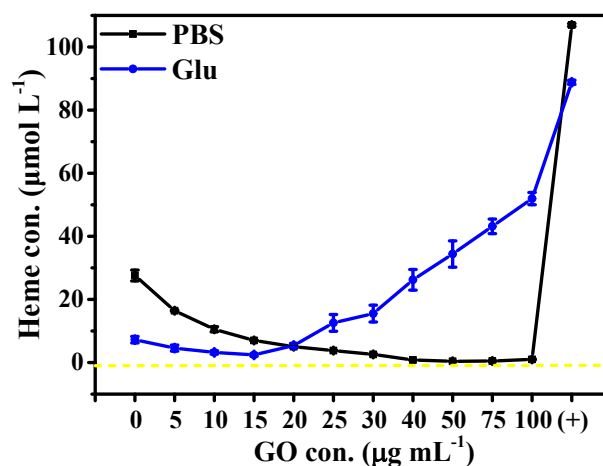


Figure S4. The heme concentration curves in two incubation media.

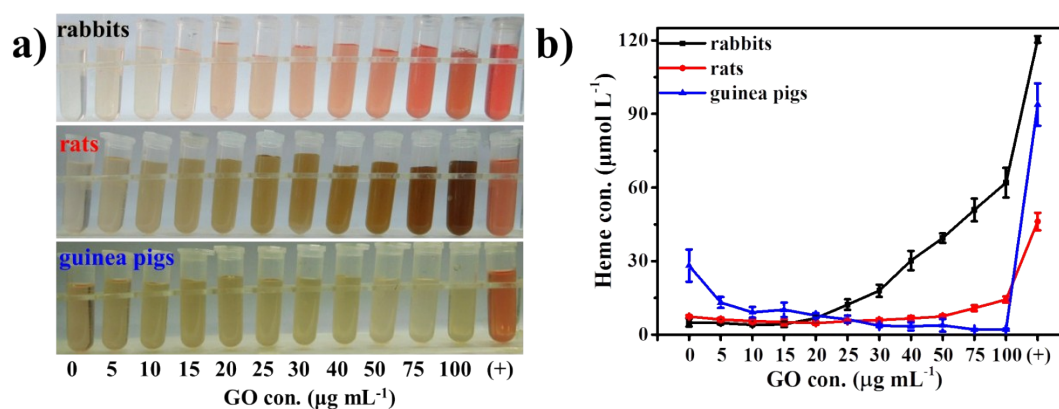


Figure S5. The effect RBCs species on hemolysis properties of GO after centrifugation. (a) Photographs of hemolytic supernatants from rabbits, rats and guinea pigs. The brown color showed the color of GO nanosheets, the red indicated free Hb in medium from intracellular RBCs. (b) The heme concentration curves from three RBCs species.

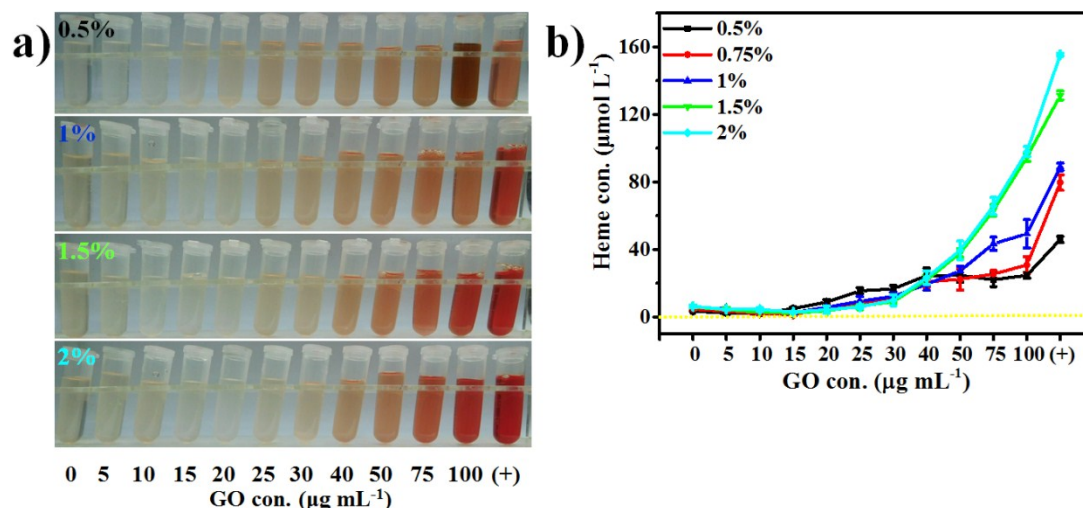


Figure S6. The effect of RBCs concentration on hemolysis of GO. (a) Photographs of hemolytic supernatants from 0.5, 1, 1.5 and 2% RBCs. (b) The heme concentration curves from five RBCs concentrations. No picture of 0.75% RBCs was a result of negligence. The free heme concentration values from five RBCs concentrations were similar to one another when GO concentration was below 15 $\mu\text{g mL}^{-1}$. The heme concentration from 0.5% RBCs was higher than the others when GO concentration was 20, 25 and 30 $\mu\text{g mL}^{-1}$. The descending order of free Hb amount was from 2% to 0.5% RBCs for the positive control and 75 or 100 $\mu\text{g mL}^{-1}$ GO.

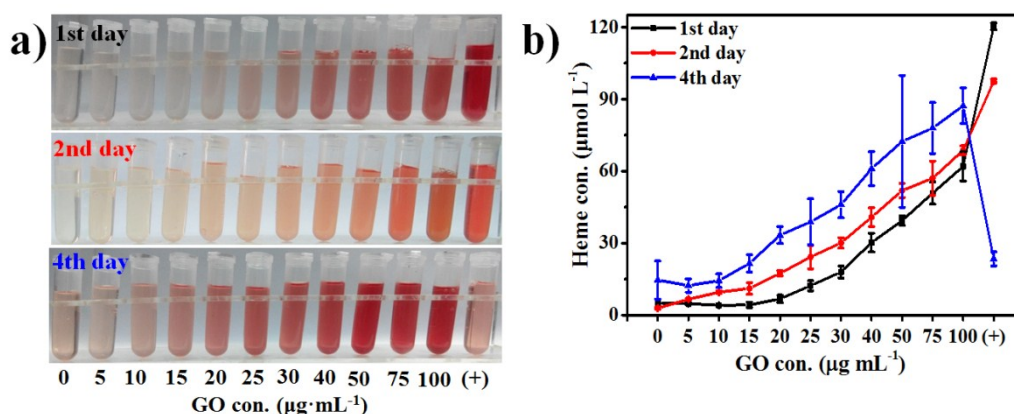


Figure S7. The storage effect of RBCs on hemolysis assays of GO. (a) Photographs of hemolytic supernatants from on the 1st, 2nd and 4th day. (b) The heme concentrations in supernatants. The hemolysis properties of GO nanosheets were relatively high for

RBCs stored three days. RBCs suffered relatively minor damage from GO nanosheets on the 1st day probably because the RBCs were most vibrant and the membranes were complete.

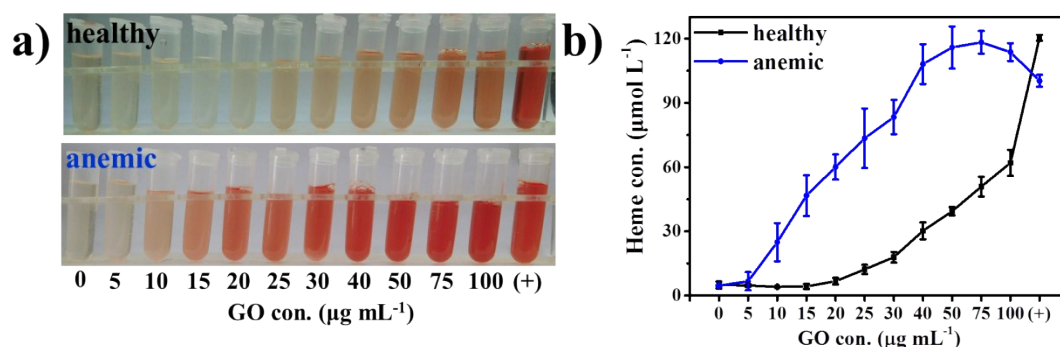


Figure S8. The health status effect of RBCs on hemolysis properties of GO. (a) Photographs of supernatants from healthy and anemic rabbits. (b) The two heme concentration curves. The increasing hemolysis from anemic rabbit blood was more intense than that from healthy blood with the increase of GO concentration. But the positive control was an opposite results. These results were illustrated that different health statuses of rabbit RBCs on hemolytic properties of GO were significant.

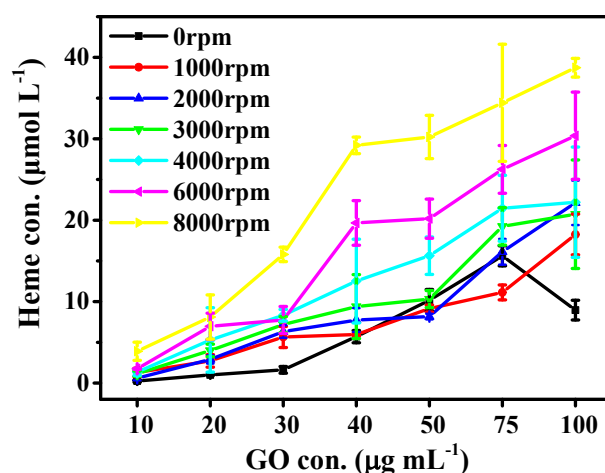


Figure S9. The centrifugal effect on hemolysis of GO. The severe hemolysis was observed at high centrifugation speed of above 4000 rpm. The centrifugation speed of 8000 rpm was showed the maximal hemolysis compared with the other speeds.

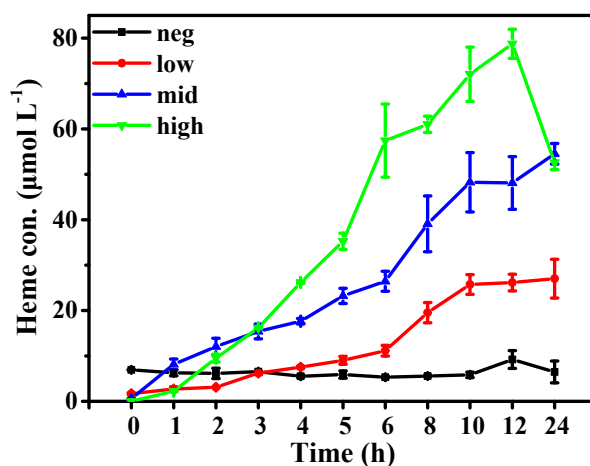


Figure S10. The heme concentration curves for the time from 0 h to 24h. An apparently increasing trend was observed at three GO concentrations (low, mid and high). However, for the negative control hemolysis was essentially constant with slight fluctuation.

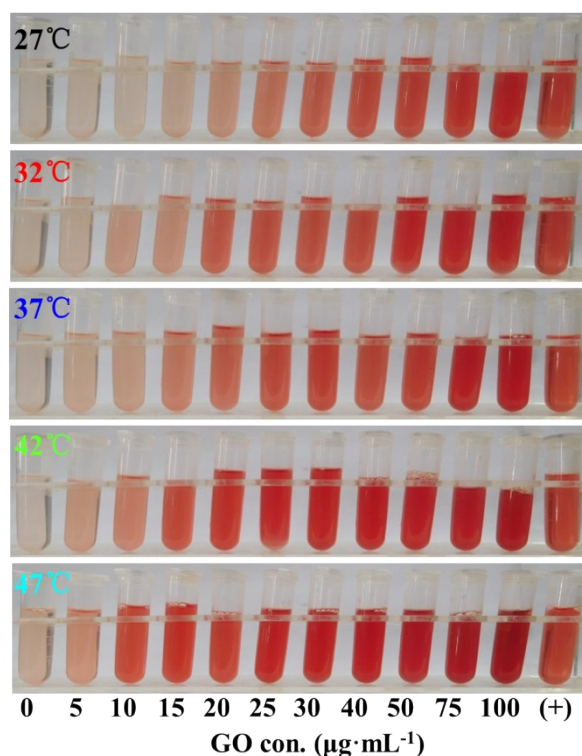


Figure S11. Photographs of hemolytic supernatants from five incubation temperatures. Apparently, serious hemolysis occurred at high GO concentration when the incubation temperature was low, while it easily caused hemolysis at low GO concentration if temperature was above 37°C.

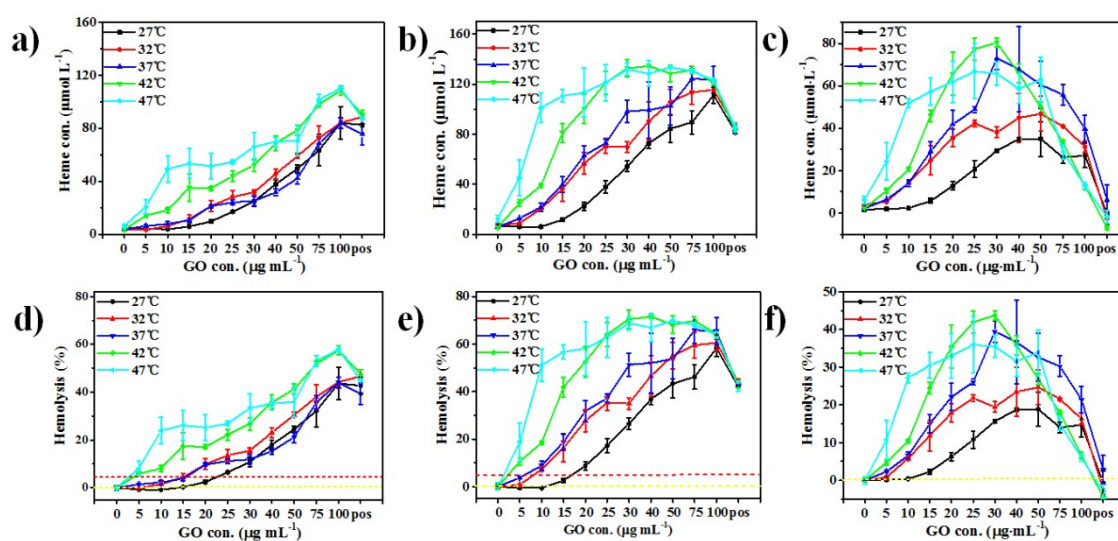


Figure S12. The incubation temperature effect on hemolysis of GO. (a), (b) and (c) were the free heme concentration curves in medium. (d), (e) and (f) were the hemolysis curves. (a) and (d) were the free heme concentration and hemolysis percentage before centrifugation, respectively. The supernatant were obtained by standing for 1 h. (b) and (e) were the free heme concentration and hemolysis percentage after centrifugation, respectively. The supernatant were obtained by centrifugation at low speed (3000 rpm for 5 min). (c) and (f) were the differences of free heme concentration and hemolysis percentage between after and before centrifugation, respectively. (c) and (f) were used to evaluate the effect of fixed centrifugation speed at different incubation temperatures.

References

1. S. K. Singh, M. K. Singh, P. P. Kulkarni, V. K. Sonkar, J. J. Gracio and D. Dash, *ACS Nano*, 2012, **6**, 2731-2740.
2. T. Wang and X. Jiang, *ACS Appl. Mater. Interfaces*, 2015, **7**, 129-136.
3. Y. Wang, A. G. El-Deen, P. Li, B. H. L. Oh, Z. Guo, M. M. Khin, Y. S. Vikhe, J. Wang, R. G. Hu, R. M. Boom, K. A. Kline, D. L. Becker, H. Duan and M. B. Chan-Park, *ACS Nano*, 2015, **9**, 10142-10157.
4. M. Guo, D. Li, M. Zhao, Y. Zhang, D. Geng, A. Lushington and X. Sun, *Carbon*, 2013, **61**, 321-328.
5. N. Ma, B. Zhang, J. Liu, P. Zhang, Z. Li and Y. Luan, *Int. J. Pharm.*, 2015, **496**, 984-992.
6. C. He, *J. Mater. Chem. B*, 2014, **3**, 592-602.

7. A. He, *RSC Adv.*, 2013, **3**, 22120-22129.
8. M. Papi, M. C. Lauriola, V. Palmieri, G. Ciasca, G. Maulucci and M. De Spirito, *RSC Adv.*, 2015, **5**, 81638-81641.
9. C. Cheng, S. Li, S. Nie, W. Zhao, H. Yang, S. Sun and C. Zhao, *Biomacromolecules*, 2012, **13**, 4236-4246.
10. X. Zhang, J. Yin, C. Peng, W. Hu, Z. Zhu, W. Li, C. Fan and Q. Huang, *Carbon*, 2011, **49**, 986-995.
11. T. Wang, *Toxicol. Res.*, 2015, **4**, 885-894.
12. B. Cai, K. Hu, C. Li, J. Jin and Y. Hu, *Appl. Surf. Sci.*, 2015, **356**, 844-851.
13. Y. Xiao, Y. Fan, W. Wang, H. Gu, N. Zhou and J. Shen, *Drug Deliv.*, 2014, **21**, 362-369.
14. S. Jin, D. Xu, N. Zhou, J. Yuan and J. Shen, *J. Appl. Polym. Sci.*, 2013, **129**, 884-891.
15. H. Zare-Zardini, A. Amiri, M. Shanbedi, A. Taheri-Kafrani, S. N. Kazi, B. T. Chew and A. Razmjou, *J. Biomed. Mater. Res. A*, 2015, **103**, 2959-2965.
16. N. Zhou, H. Gu, F. Tang, W. Li, Y. Chen and Y. Jiang, *J. Mater. Sci.*, 2013, **48**, 7097-7103.
17. J. Tan, N. Meng, Y. Fan, Y. Su, M. Zhang, Y. Xiao and N. Zhou, *Mat. Sci. Eng. C*, 2016, **61**, 681-687.
18. N. Meng, S. Q. Zhang, N. L. Zhou and J. Shen, *Nanotechnology*, 2010, **21**, 185101.
19. S. A. Love, J. W. Thompson and C. L. Haynes, *Nanomedicine*, 2012, **7**, 1355-1364.
20. R. E. Waugh, M. Narla, C. W. Jackson, T. J. Mueller, T. Suzuki and G. L. Dale, *Blood*, 1992, **79**, 1351-1358.
21. P. Montes-Navajas, N. G. Asenjo, R. Santamaria, R. Menendez, A. Corma and H. Garcia, *Langmuir*, 2013, **29**, 13443-13448.
22. A. Bersényi, S. G. Fekete, Z. Szöcs and E. Berta, *Acta Vet. Hung.*, 2003, **51**, 297-304.
23. L. B. Leverett, J. D. Hellums, C. P. Alfrey and E. C. Lynch, *Biophys. J.*, 1972, **12**, 257-273.